Food Chemistry 190 (2016) 912–921

Contents lists available at ScienceDirect

Food Chemistry

journal homepage: www.elsevier.com/locate/foodchem

The mechanism of hydrothermal hydrolysis for glycyrrhizic acid into glycyrrhetinic acid and glycyrrhetinic acid 3-*O*-mono-β-D-glucuronide in subcritical water

Rui Fan, Nan Li, Honggao Xu, Jun Xiang, Lei Wang, Yanxiang Gao *

Beijing Key Laboratory of Functional Food from Plant Resources, College of Food Science & Nutritional Engineering, China Agricultural University, Beijing 100083, PR China

ARTICLE INFO

Article history:
Received 15 February 2015
Received in revised form 15 May 2015
Accepted 15 June 2015
Available online 16 June 2015

Chemical compounds studied in this article:
Glycyrrhizic acid (PubChem CID: 14982)
Glycyrrhetinic acid (PubChem CID: 10114)

Keywords:
Hydrolysis
Glycyrrhizic acid
Glycyrrhetinic acid
Glycyrrhetinic acid 3-*O*-mono-β-D-glucuronide
Subcritical water

ABSTRACT

To improve the bioactivity and sweetness properties of glycyrrhizic acid (GL), the hydrothermal hydrolysis of GL into glycyrrhetinic acid (GA) and glycyrrhetinic acid 3-*O*-mono-β-D-glucuronide (GAMG) in subcritical water was investigated. The effects of temperature, time and their interaction on the conversion ratios were analyzed and the reactions were elaborated with kinetics and thermodynamics. The results showed that GL hydrothermal hydrolysis was significantly ($P < 0.05$) affected by reaction time and temperature, as well as their interaction, and could be fitted into first-order kinetics. The thermodynamic analysis indicated that the hydrolysis of GL was endergonic and non-spontaneous. The hydrolytic pathways were composed of complex consecutive and parallel reactions. It was concluded that subcritical water may be a potential medium for producing GAMG and GA.

1. Introduction

Liquorice has been widely used in Chinese traditional medicine to cure phthisis, contagious hepatitis and bronchitis based on its anti-inflammatory, antiviral and antineoplastic properties (Wang & Yang, 2007). There are more than 400 compounds separated from different Glycyrrhiza species, and triterpene saponins are proven to be the major component (Cinatl et al., 2003).

Glycyrrhizic acid (GL), composed of one molecule of aglycone with two molecules of glucuronic acid (Fig. 1a), is a natural sweetener in liquorice (Cinatl et al., 2003) and has been widely used in the tobacco, food and pharmaceutical industries (Wang et al., 2012). GL also possesses many useful pharmacological activities, such as anti-cancer, anti-inflammatory and anti-bacterial properties (Zhang & Ye, 2009). However, as a bioactive compound, GL is not an optimal molecule for absorption in the bloodstream and disturbs ionic metabolic equilibrium in many organisms, which can cause hypertension (Cinatl et al., 2003).

Glycyrrhetinic acid (GA), the aglycon of GL, is produced by GL hydrolysis, which removes two molecules of glucuronic acid moieties. GA is a component of liquorice, which can be completely hydrolyzed by intestinal bacteria and enter into the body's systematic circulation (Krähenbühl, Hasler, & Krapf, 1994). Both GL and GA can inhibit the proliferation of hepatoma carcinoma cells, with the dose of GA only 2.5% of GL to obtain an equal effect (Zhang & Ye, 2009). In addition, GA has a more significant effect on *in vitro* anti-platelet aggregation compared to GL. GA also exhibits cytotoxicity against tumor cells as well as inhibitory activities on rotavirus infections (Kim et al., 2000). Therefore, GA has some advantages over GL (Farese et al., 2009), and is considered as a promising lead compound for designing a more efficacious and less toxic chemosensitizing agent to enhance the efficacy of cancer chemotherapy (Maatooq, Marzouk, Gray, & Rosazza, 2010).

Glycyrrhetinic acid 3-*O*-mono-β-D-glucuronide (GAMG) is formed after cleaving the distal glycosidic bond of GL (Fig. 1a), and has a higher bioactivity, stronger physiological function, more pleasant sweetness and a lower caloric value compared to those of GL (Ohtake et al., 2007). As a sweetener, its sweetness intensity is 5-fold higher than that of GL, and GAMG is much safer as its

* Corresponding author at: Box 112, No. 17 Tsinghua East Rd., Haidian District, Beijing 100083, China.
E-mail address: gyxcau@126.com (Y. Gao).

http://dx.doi.org/10.1016/j.foodchem.2015.06.039
0308-8146/

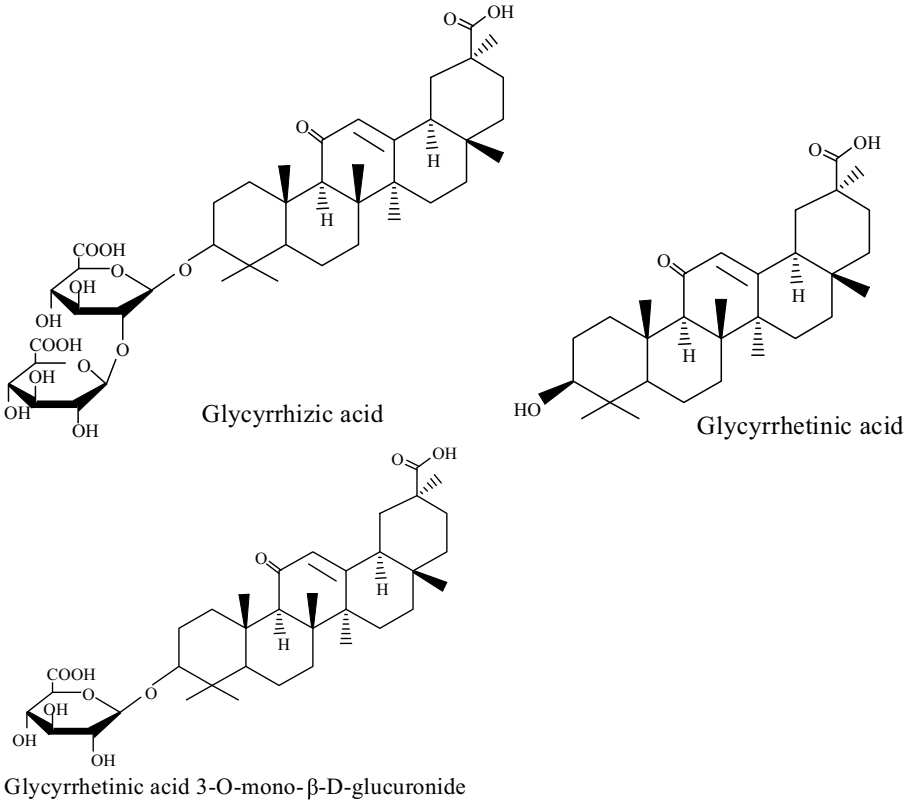

(a)

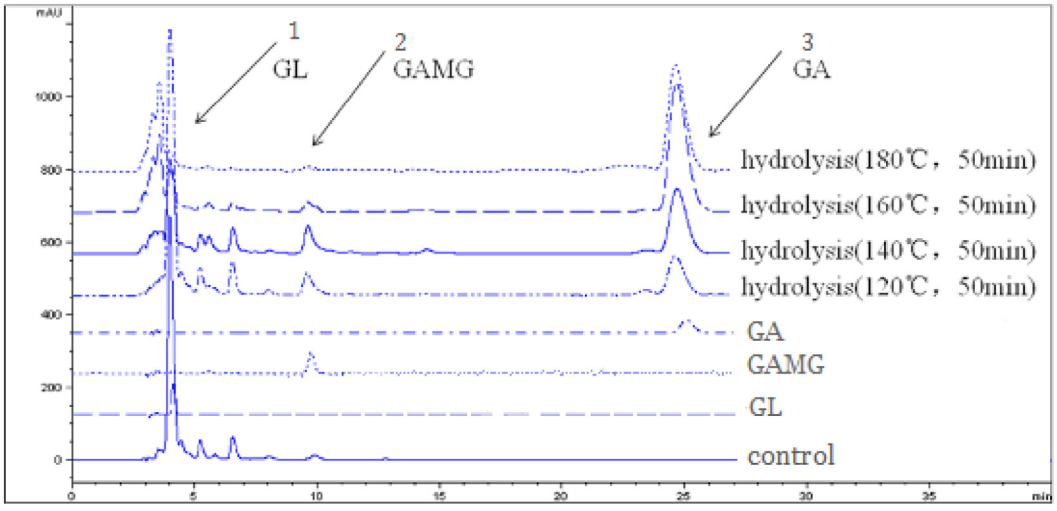

(b)

Fig. 1. HPLC profiles of compounds in hydrolysate of GL, (a) the structures of glycyrrhizic acid (GL), glycyrrhetinic acid (GA) and glycyrrhetinic acid 3-*O*-mono-β-D-glucuronide (GAMG); (b) the HPLC profiles before and after hydrolysis of GL.

median lethal dose (MLD_{50}) is 5 g/kg bw, while the MLD_{50} of GL is 0.8 g/kg bw (Feng, Li, Xu, & Wang, 2006). There are many similar characteristics between GAMG and GL in drug formulation, such as antivirus, anti-inflammatory and anti-tumor properties, however, the biological availability of GAMG is higher than that of GL (Ohtake et al., 2007). Therefore, GAMG is being considered as a promising and excellent food sweetener and therapeutic agent.

GA and GAMG are traditionally hydrolyzed from GL with hot concentrated mineral acid over 10 h (Kim, Lee, & Han, 1999). GA and GAMG were also reported to be produced from GL hydrolysis with β-D-glucuronidase (Huang et al., 2009). However, the process of β-D-glucuronidase biocatalysis was difficult to realize in industrial-scale production because of its high cost, low activity and biocatalyst selectivity (He et al., 2010). In addition, the large-scale production of GAMG was limited because of the poor hydrophilicity of both GL and GAMG (Chen, Kaleem, He, Liu, & Li, 2012). It was reported that the fungus *Penicillium purpurogenum* Li-3 could produce specific β-D-glucuronidase, which possessed high chemical bond selectivity and could be directly used for producing GAMG. However, the yield of specific β-D-glucuronidase was relatively low (Feng et al., 2006). There is another method with high yield of β-D-glucuronidase, the gene pgus (GenBank Accession

No. EU095019) was cloned and over-expressed in *Escherichia coli* BL21, but its chemical bond selectivity was still lower than that from the corresponding wild strains (Song, Wang, Chen, & Li, 2008). To overcome these disadvantages of conventional chemical and biotransformation methods, especially for longer hydrolysis time, more complicated operations and a higher cost, a new method of producing GA and GAMG should be focussed.

Subcritical water (SW), a common compressed fluid, is often used as a solvent, reagent and catalyst in extractions, hydrolytic reactions and cleaning because of its decreased viscosity and surface tension, increased diffusivity and self-ionization (Carr, Mammucari, & Foster, 2011). SW was used as an environmentally friendly medium for organic compounds and biomass hydrolysis to produce useful substances, such as cellulose decomposition (Matsunaga, Matsui, Otsuka, & Yamamoto, 2008), protein aggregation, disaggregation and hydrolysis (Rogalinski, Liu, Albrecht, & Brunner, 2008), recovery of oil and free fatty acids (Fattah, Mostafa, Mahmoud, & Abdelmoez, 2014) and hesperidin hydrolysis (Ruen-ngam, Quitain, Tanaka, Sasaki, & Goto, 2012). However, there is no information on the formation of GA and GAMG from GL in SW. The purpose of the present study was to investigate the GL hydrolysis process in SW. The effects of hydrolytic temperature, time and their interaction on the conversion ratios of GA, GAMG and GA were analyzed. The GL hydrolysis was elaborated with kinetic and thermodynamic analyses, and the mechanism of GL conversion into GA and GAMG was also interpreted.

2. Materials and methods

2.1. Chemicals

Standards of GL (⩾98%) and GA (⩾98%) were purchased from Winherb Medical Science Company, Ltd. (Shanghai, China). GAMG (⩾80%) was provided by Prof. Li (bioengineering lab in Beijing Institute of Technology). All reagents (HPLC-grade) were obtained from Merck (Shanghai, China). Other chemicals and solvents (analytical-grade) were purchased from Beijing Chemical Company (Beijing, China). Crude glycyrrhizic acid (90%, based on UV method) was purchased from Fanzhi Biological Technology Company, Ltd. (Lanzhou, China).

2.2. Hydrothermal hydrolysis of GL

The hydrolytic reaction was carried out with a subcritical water extraction apparatus (Model CWYF-2, Haihua Petroleum Research Instrument Company, Ltd., Nantong, Jiangshu, China), as previously described by He et al. (2012) and Xu, Liu, Zhao, and Gao (2008). The hydrolysis was carried out at a constant pressure of 7.0 MPa. The GL solution (4 g dissolved in 100 ml 30% (v/v) ethanol solution) was purged at a constant flow rate (20 ml/min), via a liquid infusion pump (Model P6000, Beijing Chuangxin Tongheng Science and Technology Company, Ltd., Beijing, China), into the sealed reaction vessel in each run. At the end of the reaction, the reaction vessel was cooled and the hydrolysate was collected. The reaction vessel was then washed with 100 ml of 30% (v/v) ethanol solution and the operation was repeated four times. The washing liquor was combined with the hydrolysate, and this was centrifuged at 1500*g* for 5 min, and then the supernatant was collected for further analysis.

Hydrolysis in SW is not only dependent upon the temperature, but also the exposure time (Carr et al., 2011). Prior to the kinetic analysis, it was necessary to investigate the interaction of time and temperature during a hydrolysis process in SW. On the basis of preliminary experiments, the reaction experiments were carried out with full factorial experiments at different temperatures (120–220 °C) for different times (10–80 min) (a total of 48 experiments) (Chen & Liu, 2007).

Regression analysis was fitted into a high-order polynomial model, shown in Eq. (1):

$$z = \sum_{i=0}^{n}\sum_{j=0}^{n-i}\left(a_{ij}x^i y^j\right) \tag{1}$$

where z represents the response, conversion ratio, a_{ij} are the interactive coefficients, x and y represent time and temperature, respectively.

The model was estimated by ANOVA, the model and three dimensional surface response plots were expressed as fitted polynomial regression equations with Matlab software 7.0 (The MathWorks, Inc., U.S.).

2.3. Determination of GL and its hydrolytic products

The hydrolysate was separated and analyzed with an Agilent 1100 HPLC-DAD system (Agilent Technologies, Ltd., USA). Chromatographic analysis was run using a reverse-phase Agilent Zorbax Eclipse Plus column (150 mm × 4.6 mm i.d., 5 μm). The mobile phase consisted of solvent A (100% methanol) and solvent B (1.0% acetic acid in ammonium acetate solution) at a ratio of 80:20. The flow rate was 0.8 ml/min, the column temperature was kept at 35 °C and the injector volume was 20 μl. The DAD wavelength was set at 250 nm.

The yield and conversion ratios of GL, GAMG and the formation of GA were calculated using the following Eqs. (2)–(7)

$$\text{Yield}_{GL}\ (g/g) = \frac{\text{the residual mass of GL in hydrolysate}}{\text{the mass of reactant GL}} \tag{2}$$

$$\text{Yield}_{GAMG}\ (g/g) = \frac{\text{the mass of GAMG in hydrolysate}}{\text{the mass of reactant GL}} \tag{3}$$

$$\text{Yield}_{GA}\ (g/g) = \frac{\text{the mass of GA in hydrolysate}}{\text{the mass of reactant GL}} \tag{4}$$

$$\text{Conversion ratio}_{GL}\ (\%) = \frac{\text{the actual mass of GL participating hydrolysis reaction}}{\text{the mass of reactant GL}} \times 100 \tag{5}$$

$$\text{Conversion ratio}_{GAMG}\ (\%) = \frac{\text{the mass of GAMG in hydrolysate}}{\text{the theoretical mass of GAMG from GL hydrolysis} \times \text{the mass of reactant GL}} \times 100 \tag{6}$$

$$\text{Formation ratio}_{GA}\ (\%) = \frac{\text{the mass of GA in hydrolysate}}{\text{the theoretical mass of GA from GL hydrolysis} \times \text{the mass of reactant GL}} \times 100 \tag{7}$$

The theoretical mass of GAMG from GL hydrolysis is defined as the mass of 1 g GL only completely converted into 0.786 g GAMG. The theoretical mass of GA from GL hydrolysis is defined as the mass of 1 g GL only completely converted into 0.574 g GA.

2.4. Kinetic analysis

2.4.1. Kinetic model

GL was hydrolyzed via the cleaving of the distal β-1,2 glycosidic bond to form the intermediate product (GAMG), which underwent further hydrolysis of the β-1,3 glycosidic bond to produce a corresponding aglycone (GA). In this reaction, glucuronic acid was a by-product and water was in excess, therefore, glucuronic acid and water were ignored. According to previous reports (Liu, Gao, Xu, Wang, & Yang, 2008; Ruen-ngam et al., 2012; Wardhani, Vázquez, & Pandiella, 2008), the kinetic analysis of GL hydrolysis might be performed based on a general approach of the first order reaction. The rate equations for the three compounds are expressed below:

$$r_{GL} = \frac{-d[GL]}{dt} = k_1[GL] + k_3[GL] = (k_1 + k_3)[GL] \tag{8}$$

$$r_{GAMG} = \frac{d[GAMG]}{dt} = k_1[GL] - k_2[GAMG] \tag{9}$$

$$r_{GA} = \frac{d[GA]}{dt} = k_3[GL] + k_2[GAMG] \tag{10}$$

where r_{GL} is the degradation rate of GL (g s^{-1}), r_{GAMG} represents the conversion rate of GAMG (g s^{-1}) and r_{GA} represents the formation rate of GA (g s^{-1}), [GA], [GL] and [GAMG] represent the mass of GA, GL and GAMG (g), respectively, k_1, k_2 and k_3 are the kinetic constants (s^{-1}), and t is the reaction time (s).

Integral form of Eq. (8) is expressed as,

$$-\ln([GL]/[GL]_0) = (k_1 + k_3)t \quad \text{or } [GL] = [GL]_0 e^{(-k_1 t - k_3 t)} \tag{11}$$

After the rearrangement, the yield is expressed as,

$$\frac{[GL]}{[GL]_0} = y_{GL} = e^{(-k_1 t - k_3 t)} \tag{12}$$

where $[GL]_0$ represents the initial mass in the hydrolytic reaction, and y_{GL} represents GL.

To find the mass variation of GAMG and GA, the mass of GL from Eq. (8) was substituted into the differential equation governing the mass change rate of GAMG and GA:

$$\frac{d[GAMG]}{dt} + k_2[GAMG] = k_1[GL]_0 e^{(-k_1 t - k_3 t)} \tag{13}$$

$$\frac{d[GA]}{dt} = k_3[GL]_0 e^{(-k_1 t - k_3 t)} + k_2[GL]_0 \times \frac{k_1}{k_2 - (k_1 + k_3)}\left[e^{(-k_1 t - k_3 t)} - e^{(-k_2 t)}\right] \tag{14}$$

By integration of Eqs. (13) and (14), the final variations in mass of GAMG and GA are:

$$\frac{[GAMG]}{[GL]_0} = \frac{k_1}{k_2 - (k_1 + k_3)}\left(e^{(-k_1 t - k_3 t)} - e^{(-k_2 t)}\right) \tag{15}$$

$$\frac{[GA]}{[GL]_0} = \frac{k_3}{k_2(k_1 + k_3)}\left[(k_1 + k_3)e^{(-k_2 t)} - k_2 e^{(-k_1 t - k_3 t)}\right] \tag{16}$$

After the rearrangement:

$$y_{GA} = \frac{k_3}{k_2(k_1 + k_3)}\left[(k_1 + k_3)e^{(-k_2 t)} - k_2 e^{(-k_1 t - k_3 t)}\right] \tag{17}$$

$$y_{GAMG} = \frac{k_1}{k_2 - (k_1 + k_3)}\left(e^{(-k_1 t - k_3 t)} - e^{(-k_2 t)}\right) \tag{18}$$

Eq. (18) is used to interpret the time dependence yield of GAMG from the hydrolytic reaction of GL.

2.4.2. Estimation for the maximum yield of GAMG

When the GAMG decomposition and production rates are equal, there is no change in GAMG content, the yield of GAMG reaches the maximum level:

$$\frac{d[GAMG]}{dt_m} = k_1[GL] - k_2[GAMG] = 0 \tag{19}$$

where t_m is the reaction time attaining the maximum yield of GAMG (s).

After the rearrangement in Eqs. (11) and (15):

$$k_1[GL]_0 e^{-(k_1 + k_3)t_m} - \frac{k_1 k_2 [GL]_0}{k_2 - (k_1 + k_3)}\left(e^{-t_m(k_1 + k_3)} - e^{-k_2 t_m}\right) = 0 \tag{20}$$

t_m is expressed as:

$$t_m = \frac{\ln\left(\frac{k_1 + k_3}{k_2}\right)}{k_1 + k_3 - k_2} \tag{21}$$

After substituting Eq. (21) into Eq. (18), the maximum yield of GAMG is expressed as:

$$y_{GAMG,m} = \frac{k_1\, e^{-(k_1 + k_3)t_m}}{k_2} \tag{22}$$

2.5. Thermodynamic analysis

The Arrhenius law, founded on empirical observations, is a common approach for estimating the relationship between reaction rate constant and temperature (Abdelmoez, Nakahasi, & Yoshida, 2007). The Arrhenius equation is expressed as follows:

$$k = A e^{(-Ea/RT)} \tag{23}$$

after taking a logarithm for both sides of Eq. (23):

$$\ln k = -Ea/RT + \ln A \tag{24}$$

where A represents the pre-exponential factor, Ea represents the activation energy, T represents the absolute temperature (K) and R is the gas constant (8.31451 J mol^{-1} K^{-1}).

In addition, thermodynamic analysis was carried out for estimating the thermodynamic parameters, enthalpy ($\Delta H^{\#}$), entropy ($\Delta S^{\#}$) and Gibb's free energy of activation ($\Delta G^{\#}$). Eyring (1935) developed the activation complex theory (ACT), which is used to estimate thermodynamic parameters in terms of the rate constant. The theory is based on transition-state theory, which proposes that any chemical reaction carried out via an intermediate structure (called the activated complex) with transitory energies between reactants and products, the intermediate structure is in a quasi-equilibrium status with the reactants during the reaction (Fattah et al., 2014).

The Eyring equations are as follows:

$$k = (kbT/h)\, e^{-\Delta G^{\#}/RT} \tag{25}$$

$$k = (kbT/h)\, e^{-\Delta S^{\#}/R}\, e^{-\Delta H^{\#}/RT} \tag{26}$$

where k represents the rate constant, kb represents the Boltzmann constant (1.380658×10^{-23} J K^{-1}) and h represents Planck's constant ($6.6260755 \times 10^{-34}$ J s).

On taking a logarithm for both sides of Eq. (26):

$$\ln(k/T) = [\ln(kb/h) + (\Delta S^{\#}/R)] - \Delta H^{\#}/RT \tag{27}$$

The Gibbs free energy of activation can be estimated by:

$$\Delta G^{\#} = \Delta H^{\#} - T\Delta S^{\#} \quad (28)$$

2.6. Statistical analysis

All the experiments and measurements were performed in triplicate. Analysis of variance (ANOVA) was performed using Matlab 7.0 (The MathWorks, Inc., U.S.).

3. Results and discussion

3.1. Hydrolysis of GL

The results of the HPLC profiles for the hydrolysate are shown in Fig. 1(b). GAMG and GA were generated in the hydrolyzate at a temperature of over 100 °C. With the rise of hydrolytic temperature, it was found that GL content decreased, while GAMG and GA contents increased from 120 to 140 °C. At higher temperatures, GA content still increased, whereas, GAMG content decreased. SW was used as a reaction medium for the hydrolytic reaction because of its unique characteristics, including high reactivity, self-ionization and autocatalysis, which led to hydrolyzing the ester and ether bonds contained in the polymer chains. During the reaction process, SW could act as an acid, being a reactant and catalyst (Siskin & Katritzky, 2000). High temperature and pressure, as well as acidic fluid, could provide positive energy to break the glucosidic bond to form GA and GAMG (Tikhomirova et al., 2010).

3.2. The effect of different parameters (time and temperature) on the GL and GAMG conversion ratios and the GA formation ratio

Fig. 2(a) shows the effect of the reaction time on the GL and GAMG conversion ratios and the GA formation ratio. The GL conversion ratio was closely dependent on reaction time; it always was increased significantly ($P < 0.05$) with the extension of time, reaching 96.1% by 210 min, which meant that GL was completely hydrolyzed. The GA formation ratio was significantly ($P < 0.05$) increased until 120 min and then remained constant, this phenomenon is in accordance with a previous report (Tikhomirova et al., 2010), which implied that a longer reaction time would result in the decomposition of aglycone (Zhang & Ye, 2009). According to Fig. 2(a), the GAMG conversion ratio was significantly ($P < 0.05$) increased from 10 min to 50 min and then kept constant. With the further extension of time (more than 90 min), the GAMG conversion ratio was significantly ($P < 0.05$) decreased due to its decomposition to form GA.

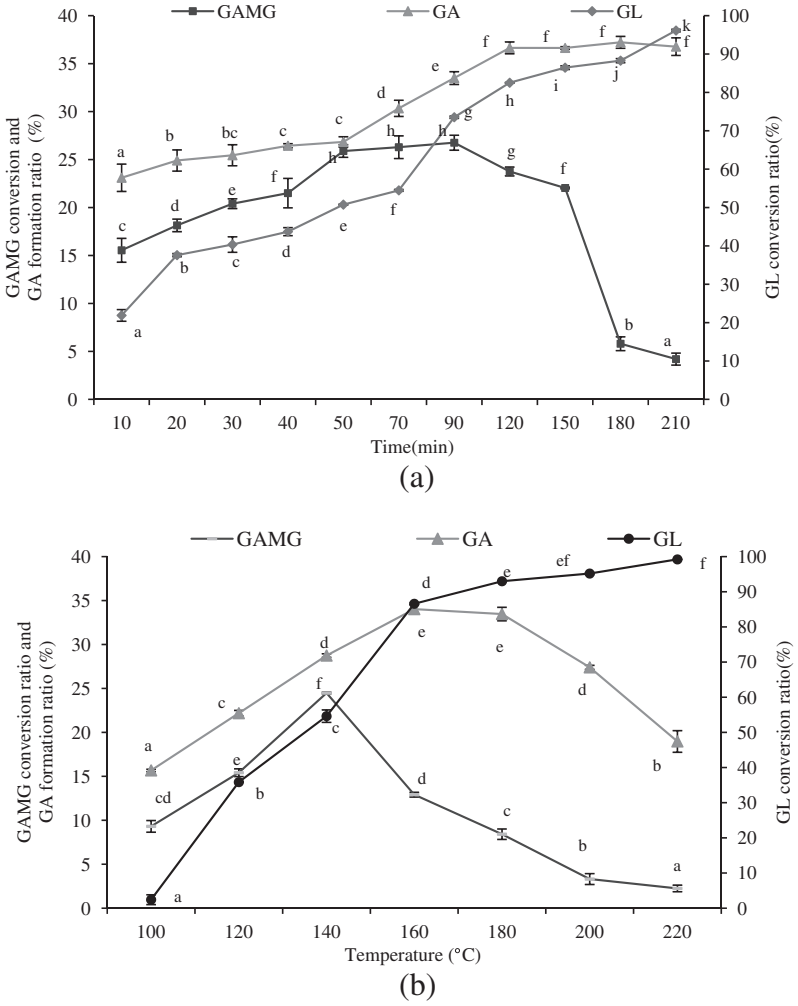

Fig. 2. The effects of time and temperature on the conversion and formation ratios, (a) the effect of time on the GL, GAMG conversion ratios and GA formation ratio[a]; (b) the effect of temperature on the GL, GAMG conversion ratios and GA formation ratio[b]. [a]The hydrolysis reactions were carried out at temperature of 140 °C under 7 MPa for different times. [b]The hydrolysis reactions were carried out under 7 MPa for 70 min at different temperatures.

Fig. 2(b) shows the effect of the temperature on the GL and GAMG conversion ratios and the GA formation ratio. The GL conversion ratio was dependent on the reaction temperature. With the rise of reaction temperature, the GL conversion ratio was significantly ($P < 0.05$) increased. At 220 °C the GL conversion ratio reached 99.1%, which meant that the GL hydrolysis was almost complete. As the temperature rose, the GAMG conversion ratio first of all increased significantly ($P < 0.05$) and then sharply decreased. The maximum conversion ratio (24.5%) of GAMG was obtained at 140 °C. As GAMG accumulated, glucoside bonds were readily hydrolyzed to form GA due to its instability at high temperatures. The GA formation ratio was increased linearly with the temperature up to 160 °C, its formation ratio reached 34% and then decreased. This could be due to higher temperatures leading to some undesirable reactions of GL, such as carbonization (Tikhomirova et al., 2010). In addition, GA also decomposed at higher temperatures. These results are in agreement with literature (Güçlü-Üstündağ, Balsevich, & Mazza, 2007). The appropriate temperature for producing GA was similar to that of a pressured microwave-assisted hydrolysis of crude glycyrrhizic acid, which was at a temperature of 150 °C for 22 min. Compared with subcritical water technology, its time was shorter, this might be due to H_2SO_4 used as a catalyst in pressured water with microwave-assist hydrolysis (Wang et al., 2012).

3.3. The effect of the interaction between reaction temperature and time on the GL and GAMG conversion ratios and the GA formation ratio

Using other preliminary experiments, hydrolytic reactions at different times (10–80 min) and temperatures (120–220 °C) were performed to evaluate the effects of both the independent variables and the interaction between them in the hydrolytic reaction process. Regression analysis and ANOVA were used for fitting into the model and estimating the significance. The ANOVA results showed that the effects of time and temperature, as well as their interaction, were very significant ($P < 0.0001$). The regression equations, high-order polynomial model, were well-fitted into all the independent variables ($R^2 > 0.85$) and their coefficients demonstrated that reaction temperature was the dominating factor. This conclusion is in agreement with the report of Zhu et al. (2010).

$$z_{GL} = -685.4 + 1.882x + 10.57y - 0.0286x^2 - 0.0524y^2 + 0.0007xy + 1.7 \times 10^{-4}x^3 + 9.2 \times 10^{-5}y^3 + 4.0 \times 10^{-6}x^2y - 4.4 \times 10^{-5}xy^2$$

$$z_{GAMG} = -565.9 + 4.296x + 9.439y - 0.0093x^2 - 0.0493y^2 - 0.0451xy - 1.9 \times 10^{-5}x^3 + 8.3 \times 10^{-5}y^3 + 5.9 \times 10^{-5}x^2y + 1.1 \times 10^{-4}xy^2$$

$$z_{GA} = 36.79 - 14.92x - 19.7y - 13.89x^2 - 2.447y^2 - 8.154xy + 6.912x^3 + 10.35y^3 + 13.22x^2y + 7.835xy^2 + 2.85x^4 + 0.281y^4 + 0.986x^3y + 2.541x^2y^2 - 1.163xy^3 - 5.026x^5 - 2.262y^5 - 2.826x^4y - 3.128x^3y^2 - 1.846x^2y^3 - 0.149xy^4$$

Fig. 3(a) shows a response surface plot with the effects of time, temperature and their interaction on the GL conversion ratio. The reaction temperature had a positive linear effect on the GL conversion ratio ($P < 0.001$). With the rise of temperature, the GL conversion ratio was consecutively increased over a short period of time; however, for a longer period of time the GL conversion ratio was firstly increased then remained constant. The linear increase in the GL conversion ratio with an extension of time was observed

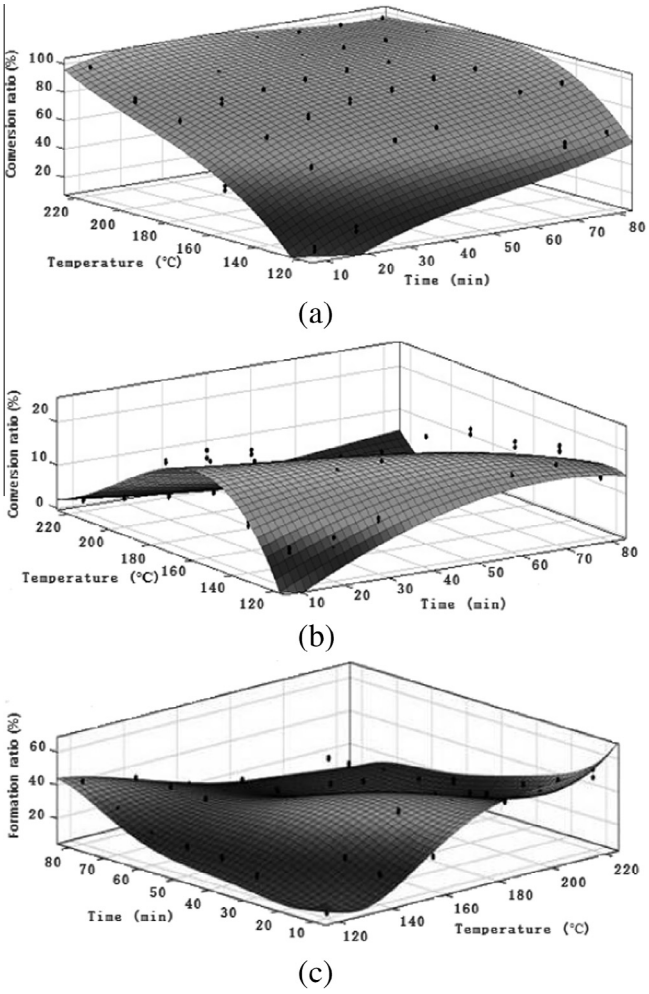

Fig. 3. The effects of time, temperature and their interaction on the conversion and formation ratios, (a) the relationship of GL conversion ratio with time and temperature; (b) the relationship of GAMG conversion ratio with time and temperature; (c) the relationship of GA formation ratio with time and temperature.

at temperatures lower than 200 °C, however, further increases in reaction time led to the conversion ratio being kept constant at relatively higher temperatures (>200 °C). At lower temperatures GL required more time to accumulate energy to be hydrolyzed; however, at higher temperatures the hydrolysis of GL was finished in a shorter period of time.

The effects of temperature, time and their interactions on the GAMG conversion ratio are shown in Fig. 3(b). Between 120 and 160 °C, with an extension of time, the conversion ratio was increased initially and then remained constant, nevertheless at higher temperatures, the conversion ratio started to slightly decrease at the beginning of the hydrolytic reaction. The curve change with the temperature was steep, therefore the reaction temperature was the predominant factor affecting the GAMG conversion ratio. On the one hand, GAMG was formed by hydrolyzing the distal glycosidic bond and removing one molecule of glucuronide, on the other hand, GAMG was decomposed at a higher temperature, due to its instability, which also could lead to directly producing GA from GL hydrolysis. These factors would result in a decrease in the GAMG conversion ratio (Tikhomirova et al., 2010).

The effects of temperature, time and their interactions on the GA formation ratio are shown in Fig. 3(c). As an extension of time, the GA formation ratio was consecutively increased at lower temperatures (120–140 °C), while the ratio firstly increased and then

decreased at the moderate temperatures (140–180 °C). When the reaction temperature was higher than 180 °C, the GA formation ratio slightly decreased at the beginning of the hydrolytic reaction. The GA formation ratio changed with temperature firstly increased and then decreased in a shorter period (<50 min), whereas the GA formation ratio was always decreased slightly over longer times (>50 min). This phenomenon was also reported in the literature (Vicente, Salagre, Cesteros, Medina, & Sueiras, 2010). It is well known that the temperature was one of the principal factors in controlling chemical reactions by directly influencing equilibrium and reaction rate constants (Kruse & Dinjus, 2007). A high level of GA formation ratio was obtained at higher temperature in a shorter time, for instance, 220 °C for 10 min or at lower temperature in a longer time, for example, 120 °C for 80 min. A longer holding time at a higher reaction temperature caused some undesirable reactions, such as carbonization, which was evident by the visible brown color of the hydrolysate and emission of a scorched flavor, a similar result was also reported by Wang et al. (2012).

3.4. The kinetic analysis of the GL hydrolytic reaction

3.4.1. Reaction pathways and mechanism

The GL hydrolysis scheme is shown in Fig. 4(a), which is composed of two parallel reactions. One is a consecutive irreversible reaction via producing an intermediate product (GAMG) and then further decomposing into GA. The other is the direct formation of GA by cleaving of the β-1,3 glycosidic bond, removing two molecules of glucuronic acid from GL. The main by-product of the hydrolytic reaction was glucuronic acid. This pathway of reaction was similar to the proposed metabolic pathway of GL by human intestinal bacteria (Kim et al., 2000).

It was suggested that the hydrolysis mainly occurred by the attacking of a proton ion dissociated from subcritical water. The oxygen atoms in the glycosidic bond were protonized, the glycosidic bond was broken and then formed the intermediates which appeared in glycosyl positive ions form or half-chair structure, and then glucuronic acid was formed by bonding OH^- dissociated from subcritical water, releasing the hydrion and acting as a catalyst (Haghighat Khajavi, Ota, Kimura, & Adachi, 2006). Fig. 3(b) shows the reaction mechanism, the breakage of the glycosidic bond was carried out in three steps, listed as follows (Sasaki, Furukawa, Minami, Adschiri, & Arai, 2002):

(1) The oxygen atom in the glycosidic bond was attacked by H^+, which led to its rapid protonation (procedure A).
(2) The positive charge was transferred to C_1 of glucuronic acid, and then a carbenium ion was formed due to the breaking of the C–O bond, and a hydroxyl group was provided to the C_2 of another glucuronic acid or C_3 of pentacyclic triterpene (procedures B and C).
(3) Subcritical water delivered OH^- to the carbenium ion, forming glucuronic acid residues, releasing H^+ (procedure D).

3.4.2. Kinetic analysis

The changes in GL, GAMG and GA content during the hydrolytic reactions were measured for the kinetic analysis. The experimental data were correlated well with the irreversible consecutive first order theoretical models estimated using Eq. (18), the values of R^2 were 0.9606, 0.9803, 0.9718, 0.9868, 0.9951 and 0.9835, respectively. It could be concluded that the GL hydrolysis was considered to be first-order reaction. Similar results were mentioned in previous reports (Liu et al., 2008; Ruen-ngam et al., 2012; Wardhani et al., 2008)

The rate constants (k_i) were affected by the temperature, and the results are shown in Fig. 5(a). With the rise in temperature, k_1 and k_2 initially increased, and then decreased, while k_3 always increased. When k_1 and k_2 started to decrease at a higher temperature (180 °C), k_3 sharply increased from 0.00182 to 0.00404 s^{-1}, which indicated that high temperatures resulted in the hydrolysis of GL. The value of k_3 was considerably larger than k_1 and k_2, which implied that the direct formation of GA was predominant. This was similar with literature, which stated that GL was metabolized to GA as a main product and GAMG as a minor product by human intestinal microflora (Kim et al., 2000). At lower temperatures of 120–180 °C, k_1 was larger than k_2, implying that the GAMG formation rate was faster than that of decomposition, which promoted GAMG to accumulate. At a lower temperature, the value of k_1 was bigger than k_2 and the GAMG yield was higher. When the difference between the k_1 and k_2 values appeared to be at the largest value at 160 °C, the GAMG yield reached a maximum level. However, with the rise of temperature, k_2 was increased at a rate faster than k_1, when the curves of k_1 and k_2 were intersected at 180 °C, k_2 was larger than k_1 due to GAMG decomposition.

The reaction times for attaining the maximum GAMG yield (t_m) at different temperatures and the corresponding yields are listed in Table 1(a). It was observed that the highest yield of GAMG was obtained by GL hydrolysis at 160 °C for 16 min; the yield was insignificantly different from that obtained at 140 °C for 74 min. Considering the cost, the parameters of 160 °C for 16 min were preferred to produce GAMG. The time for producing GAMG in subcritical water was much shorter than that of other methods, such as the biosynthesis in a water-miscible ionic liquid by immobilizing whole cells of *P. purpurogenum* Li-3, where the optimal time was 62 h in ionic liquid co-solvent medium compared to 72 h in buffer medium (Chen et al., 2012). It was concluded that subcritical water technology for the preparation of GAMG and GA was the efficient and green technology.

3.5. Thermodynamic analysis

The Arrhenius equation is a common method for analyzing the relationship between the reaction rate and temperature. Due to the k_1 and k_2 being decreased at a higher temperature, the estimation of the Arrhenius parameters was carried out below 180 °C. To evaluate the Arrhenius parameters, the logarithmic values of the rate constants (k_i) were calculated, and the results are showed in Fig. 5(b). The estimated values are listed in Table 1(b).

In consecutive reactions, the activation energies (*Ea*) of the reactions 1 and 2 were 61.112 kJ/mol and 129.521 kJ/mol, respectively. This indicated that the energy barrier for the cleavage of the β-1,2 glucosidic bond would be lower than that of the β-1,3 glucosidic bond. The higher activation energy in reaction 2 led a slower clearing rate of the β-1,3 glucosidic bond compared to the β-1,2 glucosidic bond. This phenomenon was due to stronger steric interactions (intra- and intermolecular van der Waals repulsions), which could slow attacks on the carbocation by H^+ self-dissociated of SW (Ong et al., 2013). Compared with the hydrolysis of cellulose in SW (Sasaki et al., 2002), the activation energy of GL hydrolysis was smaller, which indicated the β-1,4- and β-1,6-glycosidic linkages in cellulose exhibited a much higher stability compared to the β-1,3- and β-1,2 glucosidic bond. The rate constants of the hydrolytic reactions were determined for the resulting monomers, and the values were found to strongly depend on the type of bonds (Rogalinski et al., 2008). The pre-exponential factor (*A*) expresses how often the molecules collide, the higher value of *A* meant a greater probability of a successful collision, which might imply the occurrence of a chemical reaction. When comparing the pre-exponential factor (*A*) between reactions 1 and 2, it can be implied that cleaving the β-1,3 glucosidic bond was more feasible than the β-1,2 glucosidic bond, however the energy required for cleaving β-1,2 glucosidic bond was lower than β-1,3 glucosidic bond. Therefore, once activated, reaction 2 proceeded quickly, even if the temperature was increased slightly.

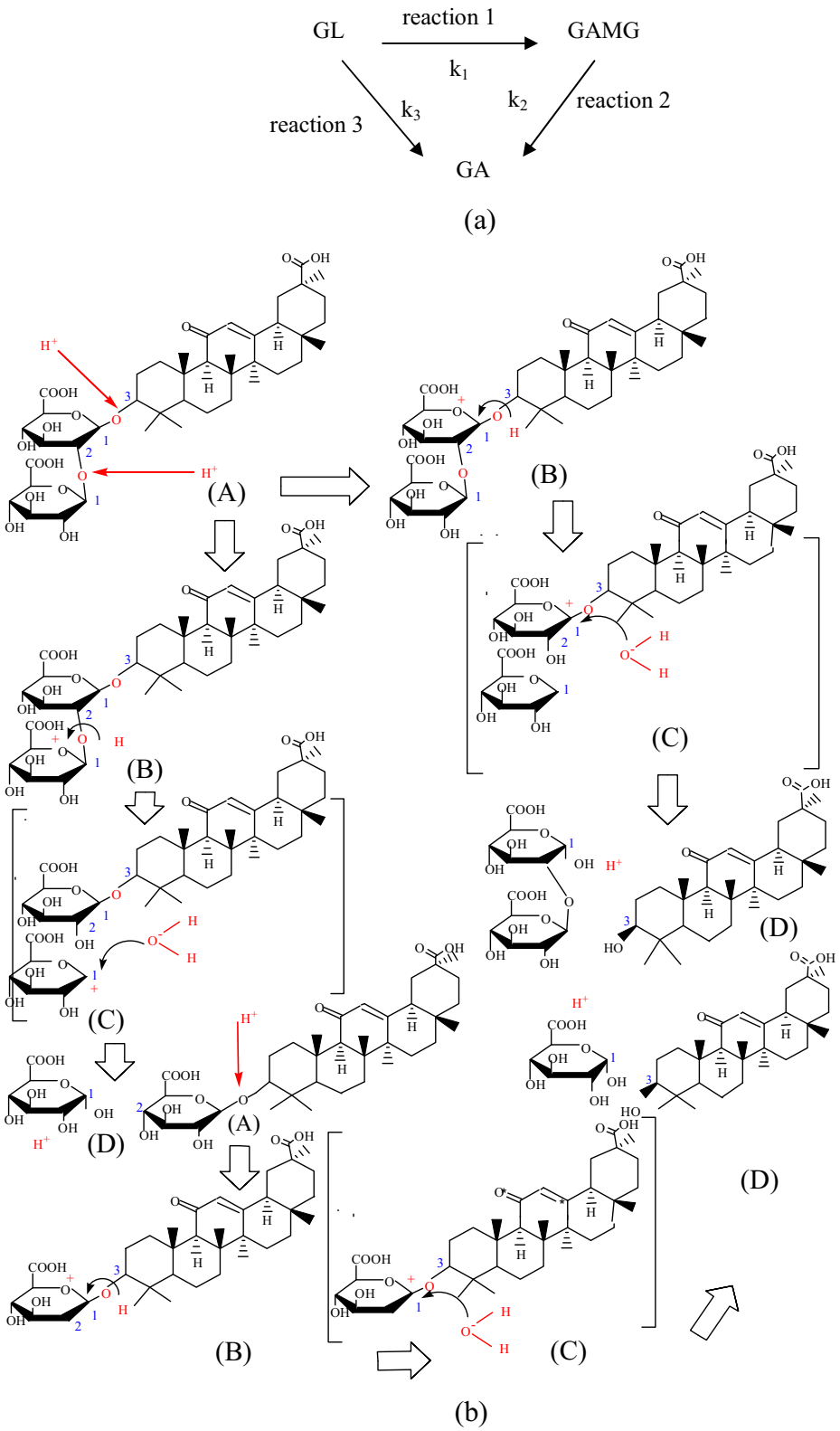

Fig. 4. Proposed reaction scheme for GL hydrolysis, (a) simplified reaction scheme for GL hydrolysis into GAMG and GA; (b) proposed major reaction pathways and mechanism of GL hydrolysis.

The obtained values for the activation energy and pre-exponential factors were within the range of reported values for the hydrothermal hydrolysis of hesperidin into hesperetin-β-glucoside and hesperetin (Ea = 83.8–143.1 kJ/mol, pre-exponential factor = 1.2×10^{11}–$1.4 \times 10^{17} s^{-1}$) (Ruen-ngam et al., 2012).

To gain a better understanding of the reaction, the thermodynamic parameters, $\Delta H^{\#}$ and $\Delta S^{\#}$ were calculated from the transition-state theory. Fig. 5(c) shows the Eyring plot for the reaction process, the values of $\Delta H^{\#}$ and $\Delta S^{\#}$ are listed in Table 1(b). The value of enthalpy ($\Delta H^{\#}$) is the amount of heat absorbed or released

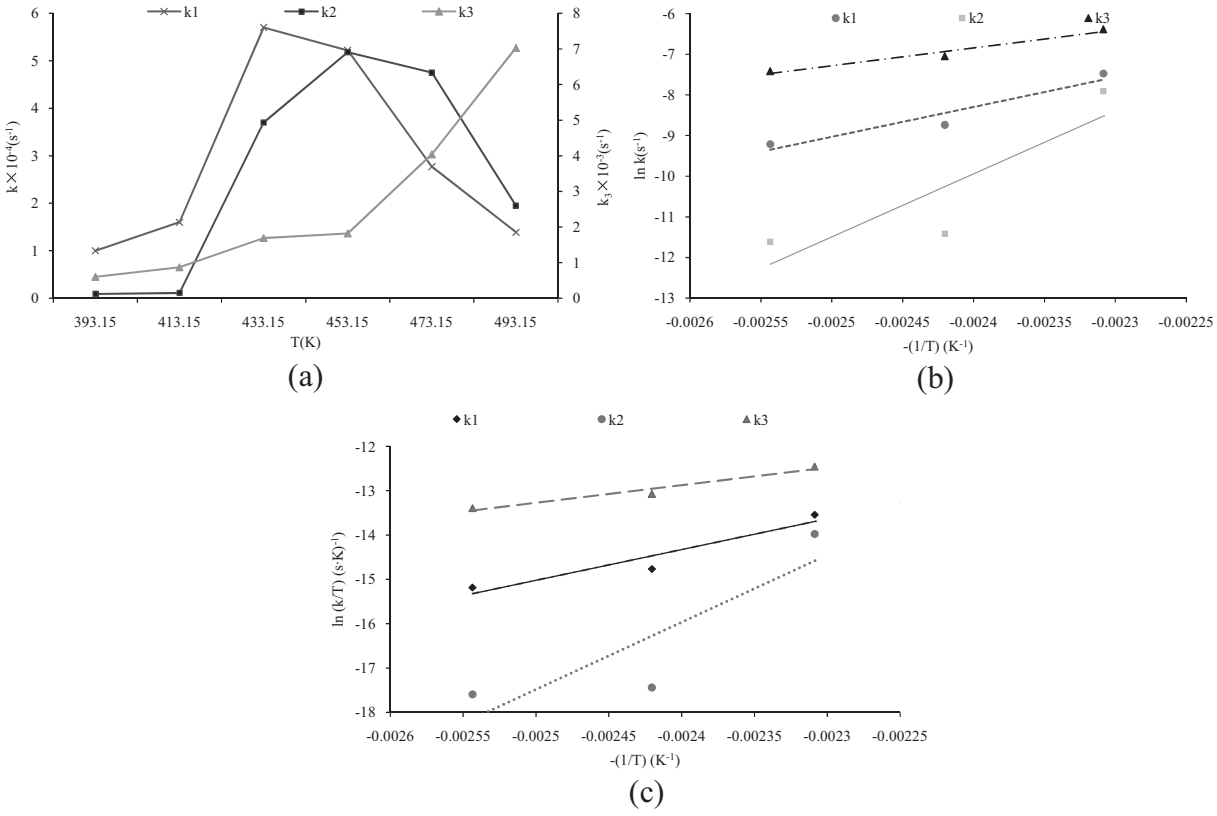

Fig. 5. The plots of estimated kinetic and thermodynamic parameters at different temperatures, (a) the reaction constants of GL hydrolysis in subcritical water; (b) the Arrhenius plots of hydrolytic reaction at different temperatures; (c) the Eyring plots of hydrolytic reaction at different temperatures.

Table 1
The summary of kinetic and thermodynamic parameters at different temperatures.

(a) Estimated t_m and GAMG yield at different temperatures

Temperature (°C)	t_m (min)	Yield (g/g)	
		Theoretical	Experimental
120	105.013	0.135[d]	0.125[e]
140	74.246	0.148[c]	0.178[a]
160	15.958	0.177[b]	0.184[ba]
180	13.786	0.145[c]	0.158[c]
200	9.574	0.049[f]	0.043[f]
220	8.614	0.018[g]	0.012[h]

(b) Estimated Arrhenius and Eyring parameters based on the data in Fig. 5

Arrhenius parameters				
Temperature (°C)	Reaction	A (s^{-1})	Ea (kJ/mol)	R^2
120–160	1	1.141×10^4	61.112	0.919
	2	8.400×10^{11}	129.521	0.764
	3	39.711	36.512	0.964
Eyring parameters				
Temperature (°C)	Reaction	$\Delta H^{\#}$ (kJ/mol)	$\Delta S^{\#}$ (kJ K^{-1} mol^{-1})	R^2
120–160	1	56.700	−0.178	0.911
	2	126.112	−0.028	0.757
	3	33.112	−0.225	0.892
Temperature/ reaction	$\Delta G^{\#}$ (kJ)			
	1	2	3	
120 °C	127.749	137.098	121.616	
140 °C	131.315	137.657	126.122	
160 °C	134.880	138.216	130.628	

in the reaction, and it indicates whether a reaction is endothermic or exothermic. $\Delta H^{\#}$ values for the three reactions were positive, which indicated that the GL hydrolysis was endothermic; it implied that energy was required to raise the energy level and convert the reactants into their transition state (Zhang, Ma, & Yang, 2004).

The value of $\Delta S^{\#}$ gives information about the degree of order in the transition state. It was found that these values were negative in all the reactions, which indicated that the transition state structure was more ordered than that of the reactant. This result is in accordance with other reports (Cho, Kim, Hong, & Yeo, 2012).

$\Delta H^{\#}$ and $\Delta S^{\#}$ values of the reaction 1 were 56.700 kJ/mol and −0.1780 kJ/(K mol), respectively, which were lower than those of reaction 2, where a low value of A corresponded to a large negative value of $\Delta S^{\#}$, indicating that unfavourable reactions occurred (Cho et al., 2012). However, the Ea of reaction 1 was lower than that of the reaction 2; therefore, the energy needed to overcome the energy barrier was lower, indicating it was easy to attain the transition state (Abdelmoez, Abdelfatah, Tayeb, & Yoshida, 2011).

Gibb's free energy of activation ($\Delta G^{\#}$) expresses the degree and spontaneity of chemical reactions. As listed in Table 1(b), the positive values of $\Delta G^{\#}$ were found in all reactions, which revealed that all the reactions were endergonic and non-spontaneous. In addition, the value of $\Delta G^{\#}$ was positive due to the higher energy level of the transition state than that of the reactant. The result explained why a high temperature was required for accelerating the hydrolytic reaction to overcome the non-spontaneous nature of the process.

4. Conclusion

Subcritical water was applied as a new medium for hydrolysis of GL into GAMG and GA. The effects of temperature, time and their interaction on the reaction rate were found to be significant ($P < 0.05$). The GL hydrolysis was composed of two parallel reactions and followed first-order kinetics. The thermodynamics

analysis indicated that SW would be efficient for GAMG and GA formation from the GL hydrolysis. The optimal parameters for producing GAMG were 160 °C for 16 min. The study provided a further understanding about GL hydrolysis in SW, which can be used as a potential design of an applicable reactor for the proposed process.

Acknowledgements

The authors acknowledge financial support from National Science-technology Support Plan Projects for the 12th five-year plan (No. 2011BAI07B02-7).

References

Abdelmoez, W., Abdelfatah, R., Tayeb, A., & Yoshida, H. (2011). Extraction of cottonseed oil using subcritical water technology. *AIChE Journal, 57*, 2353–2359.
Abdelmoez, W., Nakahasi, T., & Yoshida, H. (2007). Amino acid transformation and decomposition in saturated subcritical water conditions. *Industrial and Engineering Chemistry Research, 46*, 5286–5294.
Carr, A. G., Mammucari, R., & Foster, N. R. (2011). A review of subcritical water as a solvent and its utilisation for the processing of hydrophobic organic compounds. *Chemical Engineering Journal, 172*, 1–17.
Chen, J. Y., Kaleem, I., He, D. M., Liu, G. Y., & Li, C. (2012). Efficient production of glycyrrhetinic acid 3-O-mono-β-D-glucuronide by whole-cell biocatalysis in an ionic liquid/buffer biphasic system. *Process Biochemistry, 47*, 908–913.
Chen, H. Z., & Liu, L. Y. (2007). Unpolluted fractionation of wheat straw by steam explosion and ethanol extraction. *Bioresource Technology, 98*, 666–676.
Cho, H. J., Kim, S. H., Hong, S. W., & Yeo, Y. K. (2012). A single step non-catalytic esterification of palm fatty acid distillate (PFAD) for biodiesel production. *Fuel, 93*, 373–380.
Cinatl, J., Morgenstern, B., Bauer, G., Chandra, P., Rabenau, H., & Doerr, H. W. (2003). Glycyrrhizin, an active component of liquorice roots, and replication of SARS-associated coronavirus. *Lancet, 361*, 2045–2046.
Eyring, H. (1935). The activated complex in chemical reactions. *Journal of Chemical Physics, 3*, 63–71.
Farese, S., Kruse, A., Pasch, A., Dick, B., Frey, B. M., Uehlinger, D. E., et al. (2009). Glycyrrhetinic acid food supplementation lowers serum potassium concentration in chronic hemodialysis patients. *Kidney International, 76*, 877–884.
Fattah, R. A., Mostafa, N. A., Mahmoud, M. S., & Abdelmoez, W. (2014). Recovery of oil and free fatty acids from spent bleaching earth using sub-critical water technology supported with kinetic and thermodynamic study. *Advances in Bioscience and Biotechnology, 5*, 262–272.
Feng, S., Li, C., Xu, X., & Wang, X. (2006). Screening strains for directed biosynthesis of β-D-mono-glucuronide-glycyrrhizin and kinetics of enzyme production. *Journal of Molecular Catalysis B-Enzymatic, 43*, 63–67.
Güçlü-Üstündağ, Ö., Balsevich, J., & Mazza, G. (2007). Pressurized low polarity water extraction of saponins from cow cockle seed. *Journal of Food Engineering, 80*, 619–630.
Haghighat Khajavi, S., Ota, S., Kimura, Y., & Adachi, S. (2006). Kinetics of maltooligosaccharide hydrolysis in subcritical water. *Journal of Agricultural and Food Chemistry, 54*, 3663–3667.
He, D. M., Kaleem, I., Qin, S. Y., Dai, D. Z., Liu, G. Y., & Li, C. (2010). Biosynthesis of glycyrrhetinic acid 3-O-mono-β-D-glucuronide catalyzed by β-D-glucuronidase with enhanced bond selectivity in an ionic liquid/buffer biphasic system. *Process Biochemistry, 45*, 1916–1922.
He, L., Zhang, X., Xu, H., Xu, C., Yuan, F., Knez, Ž., et al. (2012). Subcritical water extraction of phenolic compounds from pomegranate (*Punica granatum* L.) seed residues and investigation into their antioxidant activities with HPLC–ABTS+ assay. *Food and Bioproducts Processing, 90*(2), 215–223.
Huang, H., Yu, H., Zhang, J., Kang, L., Feng, B., Song, X., et al. (2009). Biotransformation of glycyrrhizin by *Aspergillus niger*. *Biocatalysis and Biotransformation, 27*, 90–95.
Kim, D. H., Hong, S. W., Kim, B. T., Bae, E. A., Park, H. Y., & Han, M. J. (2000). Biotransformation of glycyrrhizin by human intestinal bacteria and its relation to biological activities. *Archives of Pharmacal Research, 23*, 172–177.
Kim, D. H., Lee, S. W., & Han, M. J. (1999). Biotransformation of glycyrrhizin to 18 beta-glycyrrhetinic acid-3-O-beta-D-glucuronide by Streptococcus LJ-22, a human intestinal bacterium. *Biological & Pharmaceutical Bulletin, 22*, 320–322.
Krähenbühl, S., Hasler, F., & Krapf, R. (1994). Analysis and pharmacokinetics of glycyrrhizic acid and glycyrrhetinic acid in humans and experimental animals. *Steroids, 59*, 121–126.
Kruse, A., & Dinjus, E. (2007). Hot compressed water as reaction medium and reactant: Properties and synthesis reactions. *Journal of Supercritical Fluids, 39*, 362–380.
Liu, X., Gao, Y. X., Xu, H. G., Wang, Q., & Yang, B. (2008). Impact of high-pressure carbon dioxide combined with thermal treatment on degradation of red beet (*Beta vulgaris* L.) pigments. *Journal of Agricultural and Food Chemistry, 56*, 6480–6487.
Maatooq, G. T., Marzouk, A. M., Gray, A. I., & Rosazza, J. P. (2010). Bioactive microbial metabolites from glycyrrhetinic acid. *Phytochemistry, 71*, 262–270.
Matsunaga, M., Matsui, H., Otsuka, Y., & Yamamoto, S. (2008). Chemical conversion of wood by treatment in a semi-batch reactor with subcritical water. *Journal of Supercritical Fluids, 44*, 364–369.
Ohtake, N., Kido, A., Kubota, K., Tsuchiya, N., Morita, T., Kase, Y., et al. (2007). A possible involvement of 3-monoglucuronyl-glycyrrhetinic acid, a metabolite of glycyrrhizin (GL), in GL-induced pseudoaldosteronism. *Life Sciences, 80*, 1545–1552.
Ong, L. K., Kurniawan, A., Suwandi, A. C., Lin, C. X., Zhao, X. S., & Ismadji, S. (2013). Transesterification of leather tanning waste to biodiesel at supercritical condition: Kinetics and thermodynamics studies. *Journal of Supercritical Fluids, 75*, 11–20.
Rogalinski, T., Liu, K., Albrecht, T., & Brunner, G. (2008). Hydrolysis kinetics of biopolymers in subcritical water. *Journal of Supercritical Fluids, 46*, 335–341.
Ruen-ngam, D., Quitain, A. T., Tanaka, M., Sasaki, M., & Goto, M. (2012). Reaction kinetics of hydrothermal hydrolysis of hesperidin into more valuable compounds under supercritical carbon dioxide conditions. *Journal of Supercritical Fluids, 66*, 215–220.
Sasaki, M., Furukawa, M., Minami, K., Adschiri, T., & Arai, K. (2002). Kinetics and mechanism of cellobiose hydrolysis and retro-aldol condensation in subcritical and supercritical water. *Industrial and Engineering Chemistry Research, 41*, 6642–6649.
Siskin, M., & Katritzky, A. R. (2000). A review of the reactivity of organic compounds with oxygen-containing functionality in superheated water. *Journal of Analytical and Applied Pyrolysis, 54*(1), 193–214.
Song, Z. K., Wang, X. Y., Chen, G. Q., & Li, C. (2008). Cloning and prokaryotic expression of β-glucuronidase from *Penicillium purpurogenum* Li-3. *Journal of Chemistry Industrial Engineering, 59*, 3101–3106 (Chinese).
Tikhomirova, K. S., Lekar, A. V., Borisenko, S. N., Vetrova, E. V., Borisenko, N. I., & Minkin, V. I. (2010). Synthesis of glycyrrhetinic acid by hydrolysis of licorice root extract in subcritical water. *Russian Journal of Physical Chemistry, B4*, 1125–1129.
Vicente, I., Salagre, P., Cesteros, Y., Medina, F., & Sueiras, J. E. (2010). Microwave-assisted synthesis of saponite. *Applied Clay Science, 48*, 26–31.
Wang, R., Lin, C., Liu, J., Yu, F., Gao, J., & Pan, X. (2012). Pressured microwave-assisted hydrolysis of crude glycyrrhizic acid for preparation of glycyrrhetinic acid. *Chinese Journal of Chemical Engineering, 20*, 152–157.
Wang, Y. C., & Yang, Y. S. (2007). Simultaneous quantification of flavonoids and triterpenoids in licorice using HPLC. *Journal of Chromatography B, 850*, 392–399.
Wardhani, D. H., Vázquez, J. A., & Pandiella, S. S. (2008). Kinetics of daidzin and genistin transformations and water absorption during soybean soaking at different temperatures. *Food Chemistry, 111*, 13–19.
Xu, H., Liu, X., Zhao, J., & Gao, Y. (2008). Effects of ribose to cysteine ratios on the formation of volatile compounds from the Maillard reaction in supercritical carbon dioxide. *Food Research International, 41*(7), 730–737.
Zhang, Y., Ma, L., & Yang, J. (2004). Kinetics of esterification of lactic acid with ethanol catalyzed by cation-exchange resins. *Reactive & Functional Polymers, 61*, 101–114.
Zhang, Q., & Ye, M. (2009). Chemical analysis of the Chinese herbal medicine Gan-Cao (licorice). *Journal of Chromatography A, 1216*, 1954–1969.
Zhu, G. Y., Zhu, X., Wan, X. L., Fan, Q., Ma, Y., Qian, H. J., et al. (2010). Hydrolysis technology and kinetics of poultry waste to produce amino acids in subcritical water. *Journal of Analytical and Applied Pyrolysis, 88*, 187–191.